Purvalanol A induces apoptosis and reverses cisplatin resistance in ovarian cancer

Xiaoyi Zhang*, Shasha Hong*, Jiang Yang, Jingchun Liu, Ying Wang, Jiaxin Peng, Haoyu Wang and Li Hong

Cisplatin (DDP) resistance limits therapeutic efficacy in patients diagnosed with ovarian cancer. Purvalanol A (Pur) is a novel cyclin-dependent kinase (CDK) inhibitor that has been demonstrated to induce apoptosis in various cancer cells. The present study investigated the effect of the combination treatment of Pur and DDP, and the potential anticancer mechanisms in epithelial ovarian cancer (EOC) cells *in vitro* and *in vivo*. We found that Pur enhanced the anti-tumor efficacy of cisplatin in EOC cells. The combination of Pur and DDP had more significant effects on apoptosis induction in EOC cells compared with the individual-treatment groups and the control group. We further demonstrated that the combination of Pur and DDP may trigger apoptosis and autophagy in EOC cells by inducing reactive oxygen species (ROS). And the ROS/Akt/mammalian target of rapamycin signaling pathway as a potential mechanism for the initiation of autophagy induced by combination therapy. Similar results were observed *in vivo*. These results demonstrated that Pur sensitized the response of EOC cells to cisplatin *in vitro* and *in vivo*, reversing the resistance to cisplatin in ovarian cancer. *Anti-Cancer Drugs* 34: 29–43 Copyright © 2022 The Author(s). Published by Wolters Kluwer Health, Inc.

Anti-Cancer Drugs 2023, **34**:29–43

Keywords: apoptosis, autophagy, combination treatment, cisplatin, oxidative stress, Purvalanol A

Department of Gynecology and Obstetrics, Renmin Hospital of Wuhan University, Wuhan, Hubei Province 430060, China

Correspondence to Li Hong, Department of Gynecology and Obstetrics, Renmin Hospital of Wuhan University, 238 Jiefang Rd, Wuchang District, Wuhan, Hubei 430060, China
Tel: +86 278804191182289; e-mail: dr_hongli@whu.edu.cn

*Xiaoyi Zhang and Shasha Hong contributed equally to the writing of this article.

Received 4 February 2022 **Revised form accepted** 28 June 2022

Introduction

Epithelial ovarian cancer (EOC) is the most lethal gynecologic malignancy [1]. The standard strategy of treatment for ovarian cancer includes surgery followed by platinum-based chemotherapy [2,3]. However, most patients already present with the advanced-stage disease for the first diagnosis, and the 5-year survival rate of ovarian cancer is approximately 49%, which is predominately due to relapse and chemoresistance [4]. Cisplatin (DDP) is widely applied in the clinic treatment of solid tumors including ovarian cancer [5]. Long-term application of DDP results in the development of chemoresistance and toxicity [6]. Therefore, it is of vital importance to seek novel strategies to enhance the sensitivity of EOC to conventional chemotherapeutic drugs.

Cyclin-dependent kinases (CDKs) are critical kinase family members that regulate cell cycle machinery and cell proliferation in conjunction with their counterparts, cyclins [7]. The regular activation of CDKs specifically controls each cell cycle stage to provide sufficient time for restoring DNA damage, which is essential to maintain the stability of the genome and cell survival [8]. Abnormal function of cell cycle regulators results in uncontrolled cell proliferation and may be related to chemoresistance [9,10]. Multiple studies have suggested that CDK inhibitors could be a more viable cancer treatment strategy [11–13]. Moreover, dysregulation of CDK1 or its cyclin partners was detected in various cancers [14–16]. Currently, Inhibitors targeting CDK1 have been validated in clinical trials or in-vitro experiments for multiple cancer types as well [17–19]. Purvalanol A (Pur) is a CDK inhibitor, which exerts its function by blocking the binding of CDK1 or CDK2 with their specific cyclin counterparts. Previous studies have shown that Pur could induce apoptosis in various cancer cells such as colon cancer [20], breast cancer [21], and non-small cell lung cancer cells [22]. Although there has been increasing evidence of the antitumor effects of Pur, its clear underlying mechanism has not been discovered. In particular, the interrelation between autophagy and antitumor activity of Pur in tumor cells is unclarified.

Autophagy is the major intracellular degradation system by which cytoplasmic materials are delivered to and degraded in the lysosome [23]. Substantial evidence has demonstrated that autophagy may exert multifactorial influences on the initiation and progression of cancer as

well as therapeutic intervention [24,25]. Besides, autophagy can be triggered and regulated via multiple mechanisms to exert its diverse efficacy, such as the reactive oxygen species (ROS)/Akt/mammalian target of rapamycin (mTOR) signaling pathway [26,27]. ROS acts as important molecules in various cancer cellular processes [28,29], and agents that trigger oxidative stress can be potential therapeutic strategies for cancer [30]. The Akt/mTOR signaling pathway, one of the major cellular signaling pathways, is frequently activated in human cancers [31]. Aberrant activation of this pathway has been extensively observed in various malignancies, which accelerates proliferation, promotes metastasis, and participates in the development of resistance to standard anticancer therapy as well [32–34]. Nevertheless, whether the ROS/Akt/mTOR signaling pathway is involved in the antitumor effect of Pur remains to be detected, and its effects on autophagy also need further investigation.

In the present study, we demonstrated that Pur can synergistically enhance the antitumor effect of cisplatin in ovarian cancer and thus reverses drug resistance, and such a combinational treatment has the potential to become a potent therapeutic strategy for ovarian cancer.

Materials and methods

Gene expression and survival analysis in ovarian cancer dataset

Gene profiling data of ovarian normal surface epithelial and ovarian cancer epithelial samples were downloaded from the GEO dataset. Pur-associated genes were retrieved using the GeneCards database. The intersection of ovarian cancer-related gene expression datasets (GSE14407, GSE27651, and GSE54388) was analyzed using the online tool 'GEO2R'. The intersection of Pur-associated genes in ovarian cancer with previously acquired differently expressed genes (DEGs) was performed using the R package 'ggplot2'. GEPIA (http://gepia.cancer-pku.cn/) which includes gene expression data from The Cancer Genome Atlas (TCGA) and the Genotype-Tissue Expression (GTEx) project was used to compare the expression of CDK1 in EOC tissue and normal tissues. The Kaplan–Meier (K-M) Plotter database (www.kmplot.com) was used to assess the prognostic relevance of CDK1 levels by survminer package. The representative immunohistochemical images were from the Human Protein Atlas databases (CAB003799).

Reagents and chemicals

Purvalanol A (purity ≥ 99%) was purchased from MedChemExpress (HY-18299; MCE). Pur was dissolved in dimethyl sulfoxide (DMSO, D2650; Sigma-Aldrich, Shanghai, China) and stored at −20°C. Cisplatin (DDP) (purity ≥ 99%) was purchased from MedChemExpress LLC, Shanhai, China (HY-17394; MCE). Other reagent sources are listed below: fetal bovine serum (FBS), trypsin/EDTA solution (GIBCO-BRL, Gaithersburg, Maryland, USA), RPMI-1640 (Gibco, Thermo Fisher Scientific, Waltham, Massachusetts, USA), Cell Counting Kit-8 (CCK-8) (BS350A; Biosharp), 3-methyladenine (3-MA) (HY-19312; MCE), *N*-acetyl-L-cysteine (NAC) (HY-B0215; MCE) and bicinchoninic acid (BCA) protein assay kit (Beyotime Institute of Biotechnology, Jiangsu, China).

Cell culture

The ovarian cancer cell lines SKOV3 and SKOV3/DDP were gifts from professor Ma Ding (Cancer Biology Research Center, Huazhong University of Science and Technology, China). All cell lines were authenticated by short tandem repeats profiling and tested negative for mycoplasma contamination. All cell lines were incubated in RPMI-1640 supplemented with 10% FBS and 1% streptomycin–penicillin in a humidified atmosphere with 5% CO_2 at 37°C. The resistant cell line SKOV3/DDP was added DDP to maintain the resistance, and the maintaining concentration is 2 μM. Cells were passaged no more than 6 months.

Cell proliferation assay

CCK-8 was used to evaluate the inhibitory effect of agents. Cells were seeded at 96-well plates at a density of 1×10^4 cells/well and incubated overnight. Various concentrations of Pur (0, 1, 2, 4, 8, 16, 32, and 64 μM), and DDP (0, 2, 4, 8, 16, 32, and 64 μM for SKOV3 cells and 0, 2, 4, 8, 16, 32, 64, and 128 μM for SKOV3/DDP cells) were incubated with the cells for 24 h and 48 h. In order to determine the combined effects of Pur and DDP, the EOC cells were exposed to various combinations of various concentrations of Pur (0, 4, 6, and 8 μM) and various concentrations of DDP (0, 20, 30, and 40 μM) for 24 h. Subsequently, 10 μL of CCK-8 reagent was added and the plates were incubated for 0.5–2 h in an atmosphere with 5% CO_2 at 37°C. The absorbance value (OD) at 450 nm of each well was measured with a PerkinElmerVictor3 1420 Multilabel Counter (Waltham, Massachusetts, USA).

Combination index

The combined effect of Pur and DDP on EOC cells was evaluated using the combination index (CI). The combined effect is classified as follows: $CI < 1$ represents a synergistic effect, $CI = 1$ represents an additive effect, and $CI > 1$ represents an antagonistic effect. CI analysis was performed using Calcusyn Graphing Software (Biosoft Inc., Missouri, USA).

Flow cytometric analysis of cell apoptosis

The SKOV3 and SKOV3/DDP cells were seeded into six-well culture plates for 24 h, and then treated with Pur (8 μM) or DDP (4 μM for SKOV3 cells and 30 μM for SKOV3/DDP cells) or the combination for 24 h. To assess apoptosis changes after using inhibitors, EOC cells were pre-incubated with inhibitors (3-MA or NAC) for 2 h before exposure to different agents. Then the cells were harvested, washed twice with ice-cold PBS, and

detected for apoptosis by double staining with annexin V-PE and 7-AAD in binding buffer for 15 min. Annexin V-PE/7-AAD Apoptosis Detection Kit (BD Biosciences, San Diego, California, USA) was used for apoptosis analysis. A flow cytometry-fluorescence-activated cell sorting (FACS) Calibur system (BD Biosciences, Franklin Lakes, New Jersey, USA) was used to conduct the signal collection, and then analyzed with FlowJo software (BD Biosciences).

Mitochondrial membrane potential assay

JC-1 assay kit (C2006; Beyotime Institute of Biotechnology, China) was used to detect the mitochondrial membrane potential ($\Delta\Psi m$). Cells were seeded at six-well plates at a density of 1×10^5 cells/well and incubated overnight. Then the EOC cells were exposed to Pur (8 μM) or DDP (4 μM for SKOV3 cells and 30 μM for SKOV3/DDP cells) alone or in combination for 24 h. Next, the cells were washed with PBS and incubated in a medium containing 2 mM JC-1 at 37°C for 20 min. Subsequently, the cells were directly observed under a fluorescence microscope after washing with ice-cold JC-1 buffer. For flow cytometry assessments, after exposure to different treatments for 24 h, the cells were trypsinized, collected in a medium containing JC-1, and then incubated at 37°C for 20 min. After washing with ice-cold JC-1 buffer, the cells were analyzed using a FACS Calibur flow cytometer, and FlowJo software (BD Biosciences) was used for data analysis.

Flow cytometric analysis of cell cycle

An appropriate number of cells were plated on a six-well plate (1×10^5 cells/well) for 24 h and then treated with Pur (8 μM) or DDP (4 μM for SKOV3 cells and 30 μM for SKOV3/DDP cells) alone or in combination for 24 h. Then cells were trypsinized, washed with 1× PBS, centrifuged at 2000×g for 5 min, and fixed with 75% ethanol overnight at 4°C. Then cells were centrifuged again, the supernatant was removed and cells were resuspended and digested in 150 μl RNaseA (YEASEN, Shanghai, China) (250–500 μg/ml) for 30 min at 37°C and then 150 μl PI (ANT161; Antagene, Wuhan,China) (50 μg/mL) was added at 4°C for 30 min in the dark. Each sample contained approximately 1×10^4 cells and was analyzed by flow cytometer. The cell cycle distribution was determined by a FACS Calibur flow cytometer (BD Biosciences, Franklin Lakes, New Jersey, USA), and FlowJo software (BD Biosciences) was used for data analysis.

Wound healing assay

Cells were plated in six-well plates (5×10^5 cells/plate) and incubated until reaching 90% confluence. The cell monolayer was scratched with a 200-μl sterile pipette tip and washed with PBS buffer three times. Different agents were carried out as mentioned above. Finally, photos of cell migration were taken by an Olympus inverted microscope (Olympus Corp, Tokyo, Japan) at 0, 24, and 48 h after scratching.

Colony formation assay

Cells were seeded at ~500 cells per well in six-well plates. After 24 h, cells were treated with the indicated concentrations of different agents for 72 h and were further incubated in a drugfree medium to form colonies. The medium was changed every 3 days until the cells had formed colonies that were of the appreciably right size. Finally, the plates were washed with PBS twice, fixed with methyl alcohol for 15 min, and stained with 1% crystal violet (G1014; Servicebio, Wuhan, China) for 5 min. ImageJ software was used to quantify the number of colonies.

Measurement of intracellular reactive oxygen species

Cells were seeded into six-well plates at an appropriate density (1×10^5 cells/well) for 24 h, and then treated with Pur or DDP alone or in combination as mentioned above for 24 h. The amount of ROS produced in cells was measured by *2′,7′*-dichlorodihydrofluorescein diacetate (Beyotime Biotech, Nantong, China) according to the manufacturer's instructions. Cells were stained with 10 μM DCFH-DA for 30 min at 37°C. Then, the cells were collected and washed twice with pre-chilled PBS. The fluorescence intensity was analyzed using a FACS Calibur flow cytometer (BD Biosciences, California, USA). To assess the changes in ROS after using inhibitors, cells were pretreated with 5 mM NAC for 2 h prior to exposure to compounds.

Measurement of intracellular superoxide dismutase

After total protein extraction from the EOC cells using radio immunoprecipitation assay (RIPA) buffer containing phenylmethylsulfonyl fluoride (PMSF). A BCA assay kit (Beyotime, China.) was used according to the manufacturer's instructions to detect the protein concentrations. Then the cell extract was collected for measurements of the total superoxide dismutase (T-SOD) activity by WST-1 method using the Superoxide Dismutase assay kit (Jiancheng Bio, Nanjing, China). Every specimen was added into different solutions according to the manufacturer's instructions and incubated at 37°C for 40 min. After that, 2 mL of the chromogenic agent was added and let stand for 10 min. Last, the absorbance value (OD) at 550 nm of each well was measured with a PerkinElmerVictor3 1420 Multilabel Counter (Waltham, Massachusetts, USA). The values were expressed as units per mg protein (U/mg), and one unit of SOD was defined as the amount of SOD inhibiting the rate of reaction by 50% at 25°C.

Autophagy flux analysis

EOC cells were transfected with mRFP-GFP-LC3 adenoviral vectors, which were purchased from HanBio Technology (Shanghai, China), and were cultured in a medium containing the indicated times and concentrations of Pur and DDP as designed at 37°C. Autophagy

flux observation and mounting were performed with laser scanning confocal microscopy (FV1200; Olympus Corp, Tokyo, Japan).

Western blotting

After treatment according to the subject design, total proteins were extracted using RIPA buffer containing PMSF and phosphatase inhibitors. Equal amounts of protein samples were subjected to 8–12% gel by SDS-PAGE and transferred onto polyvinylidene fluoride membranes. Membranes were blocked with 5% BSA at room temperature for 1 h and then incubated with the corresponding primary antibodies overnight at 4°C. After being washed with Tris-buffered saline with Tween-20, the membranes were incubated with horseradish peroxidase-labeled goat anti-rabbit IgG (H + L) secondary antibodies (1: 3000; Servicebio) for 1 h at room temperature. The reactive protein bands were visualized using the Molecular Imager ChemiDoc Touch Imaging System with Image Lab 5.2 quantitative assay system (Bio-Rad Laboratories, Hercules, California, USA) with BeyoECL Star (Beyotime).

The primary antibody information was as follows: anti-β-actin (1:3000, GB11001; Servicebio), anti-Beclin-1(1:1000, 11306-1-AP; Proteintech), anti-LC3 (1:1000, 14600-1-AP; Proteintech), anti-cytochrome C (1:1000, #11940; CST), anti-Bcl-2 (1:1000, ab32124; Abcam), anti-Bax (1:1000, ab32503; Abcam,), anti-CDK1 (1:1000, #4539; CST), anti-mTOR (1:1000, ab134903; Abcam), anti-p-mTOR (1:1000, YP0176; Immunoway), anti-p62 (1:1000, #23214; CST), anti-Akt (1:1000, ab8805; Abcam), anti-phospho-Akt (1:1000, #4060; CST), anti-Caspase12 (1:1000, 55238-1-AP; Proteintech), anti-cleaved-Caspase3 (1:1000, abs132005; Absin), anti-Atg16 (1:1000, 29445-1-AP; Proteintech), anti-Atg5 (1:1000, 10181-2-AP; Proteintech), and anti-Atg3 (1:1000, 11262-2-AP; Proteintech).

Tumor xenograft study

The ethical committee of the Institutional Animal Care and Use Committee of Renmin Hospital of Wuhan University approved all experimental procedures in this study, and all experimental procedures were handled according to the Guide for the Care and Use of Laboratory Animals, eighth edition. Xenograft tumor models were established in female BALB/c nude mice (nu/nu, aged 6–8 weeks) that were purchased from the Center for Animal Experiment of Wuhan University. Logarithmic growth phase SKOV3/DDP cells (1×10^7/0.2 mL) were subcutaneously injected into the right flank of each mouse. After the tumor volume reached 50 mm^3, treatment was initiated. Twenty mice were randomized into four groups (five/group) and were treated with normal saline, DDP (5 mg/kg), Pur (25 mg/kg), and Pur (25 mg/kg) +DDP (5 mg/kg) by intraperitoneal injection. All groups received their respective treatments every 3 days six total times and were observed until 24 days. Mice were sacrificed until the experiment was terminated, and tumor tissues were removed for further analysis.

Histopathology and immunohistochemistry

Tissue samples isolated from xenograft tumors were subjected to histological analysis. Tumor samples were first fixed with formalin and then embedded in paraffin, cut into 5 μm sections, and stained with H&E for immunohistochemistry (IHC) staining. The primary antibodies used were anti-LC3 (1:1000, 14600-1-AP; Proteintech), anti-p-mTOR (1:1000, YP0176; Immunoway), and anti-phospho-Akt (1:1000, #4060; CST). Images were visualized using an Olympus inverted microscope (Olympus Corp.), and image analysis was performed by ImageJ.

Statistical analysis

Statistical analysis was performed with GraphPad Prism software version 7 (San Diego, California, USA). The data are presented as mean ± SEM. Student's *t*-tests (unpaired two-tailed) were performed for comparisons in two groups, and a one-way analysis of variance was used for multiple comparisons in three or more groups. P values < 0.05 were considered significant. Statistical analysis was performed with GraphPad Prism software version 7 (San Diego, California, USA).

Results

Pur-related gene CDK1 is upregulated in ovarian cancer

We first retrieved and analyzed ovarian cancer-related gene expression datasets (GSE14407, GSE27651, and GSE54388) to filter out DEGs (Fig. 1a). In the intersection, we chose CDK1 for further research. Next, the expression of CDK1 was compared in ovarian tumors and normal ovary tissues from TCGA and GTEx databases. Compared to normal ovary tissues, the expression of CDK1 was significantly upregulated in ovarian tumors (Fig. 1b). Moreover, our data indicated that ovarian cancer patients at FIGO stage IV exhibited an increased expression of CDK1 compared to other FIGO stages (Fig. 1c). In addition, IHC staining for CDK1 protein displayed a significantly higher expression in ovarian tumors than in normal ovary tissues (Fig. 1d). As a result, we chose Purvalanol A, known as a CDK1 inhibitor, to further confirm the role of CDK1 in ovarian cancer. This was more fully demonstrated by the intersection of the Pur-related genes (from GeneCards database) in ovarian cancer with previously acquired DEGs including the CDK1 gene (Fig.1e).

Pur alone, DDP alone, and their combination inhibit the viabilities of ovarian cancer cells

In order to examine the effects of Pur and DDP individual treatment on the viability of two EOC cell lines (SKOV3 and SKOV3/DDP) *in vitro*, the cell proliferation assay was performed. EOC cells were treated with Pur and DDP at different concentrations for 24 and 48 h, respectively.

Fig. 1

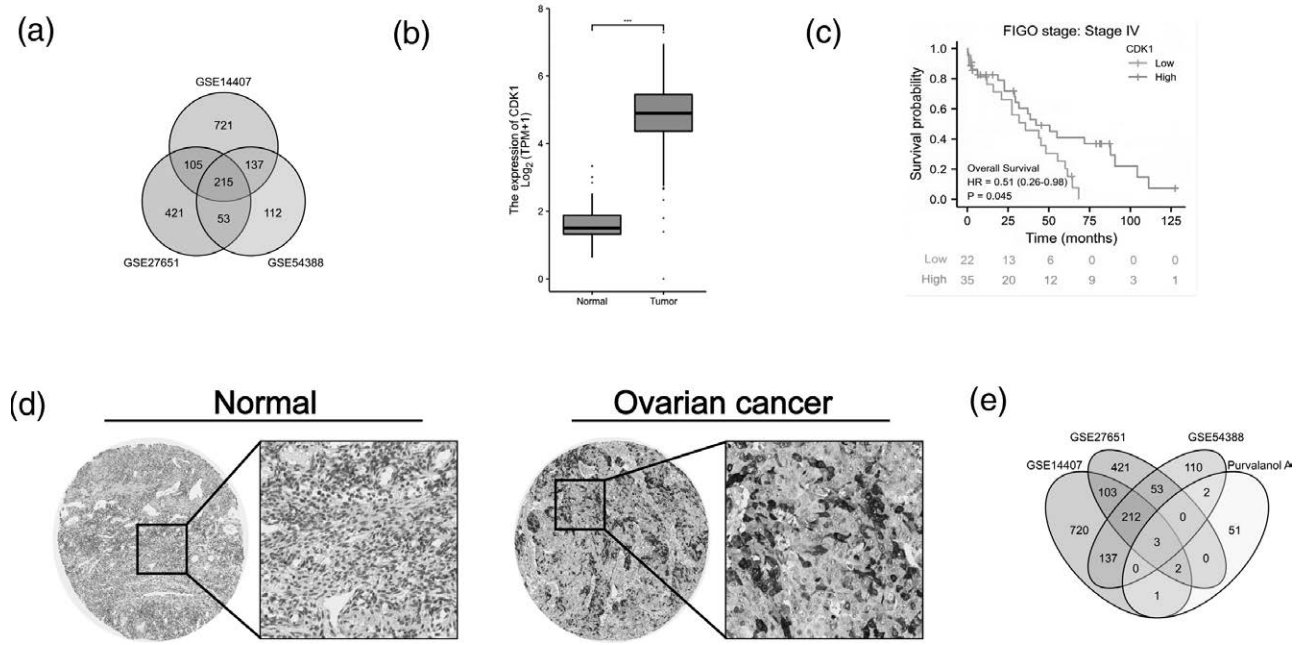

Pur-related gene CDK1 is upregulated in ovarian cancer. (a) The intersection of ovarian cancer-related gene expression datasets (GSE14407, GSE27651, and GSE54388). (b) The intersection of Pur-associated genes in ovarian cancer with previously acquired DEGs. |logFC| > 2 and *P* value < 0.05. (c) Gene expression of CDK1 in epithelial ovarian tumors and normal epithelial ovary tissues according to TCGA and GTEx databases. (d) Kaplan–Meier analysis between ovarian cancer at FIGO stage IV and CDK1 expression. (e) CDK1 was highly expressed in EOC tissues from Human Protein Atlas (https://www.proteinatlas.org) analysis. CDK1 protein was not expressed in normal ovarian tissues (https://images.proteinatlas.org/3799/10153_A_4_7.jpg), whereas high expression was observed in EOC tissues (https://images.proteinatlas.org/3799/10150_B_3_7.jpg). EOC, epithelial ovarian cancer; GTEx, Genotype Tissue Expression; TCGA, The Cancer Genome Atlas.

As shown in Fig. 2a–d, both treatments with Pur alone and DDP alone caused dose- and time-dependent loss of viability in the two EOC cell lines. The 50% inhibitory concentrations (IC50) values of Pur for SKOV3 cells were determined to be 19.690 μM and 9.062 μM at 24 h and 48 h, respectively; and for SKOV3/DDP cells, 15.920 μM and 4.604 μM. DDP IC50 values in SKOV3 cells, respectively, were 8.617 μM and 4.059 μM at 24 h and 48 h, and for SKOV3/DDP cells, 49.360 μM and 20.420 μM separately.

Subsequently, to determine whether low-toxicity concentrations of Pur might synergistically enhance DDP-induced cell growth inhibition in EOC cells, we examined the effect of Pur/DDP combination treatment on cell viability in EOC cells. The cell proliferation assay demonstrated that, compared to single DDP treatment, combination treatment with Pur remarkably decreased the viabilities of both EOC cells (Fig. 2e and f). Drug interaction of Pur and DDP was calculated by CI values, and a CI below 1 is an indication of synergism [35]. The CI results are shown in Table 1, and the vast majority of the combinations showed synergistic effects (CI < 1). Therefore, we selected 8 μM Pur and 4 μM DDP for SKOV3 cells, and 8 μM Pur and 30 μM DDP for SKOV3/DDP cells in our subsequent experiments. Afterward, the inhibitory effects on cell growth were evaluated by colony formation assay. Compared with Pur or DDP treatment alone, the combined treatment remarkably decreased the colony formation in both SKOV3 and SKOV3/DDP cells (Fig. 2*g*–i). The wound-healing assay also showed that the combination of Pur and DDP evidently decreased cell migration (Fig. 2j–l). These results demonstrated that the combination of Pur and DDP inhibited the growth and migration of EOC cells, suggesting a reversal of resistance to cisplatin.

The combination treatment of Pur and DDP induces the apoptosis of ovarian cancer cells

Next, to address whether co-treatment could result in cellular apoptosis, annexin V-PE/7-AAD double staining was performed by flow cytometric analysis. As shown in Fig. 3a–d, compared with single-agent treatment, the combined treatment dramatically increased apoptotic cell death in both SKOV3 and SKOV3/DDP cells. We then detected the expression levels of apoptosis-related proteins by western blotting. As shown in Fig. 3e, compared to the control and single-agent groups, the expression levels of proapoptotic proteins, such as cleaved caspase-3, Bax, and cytochrome-C, were significantly upregulated in both EOC cell lines, accompanied by a dramatic downregulation of the antiapoptotic protein Bcl-2 after Pur/DDP co-treatment.

Fig. 2

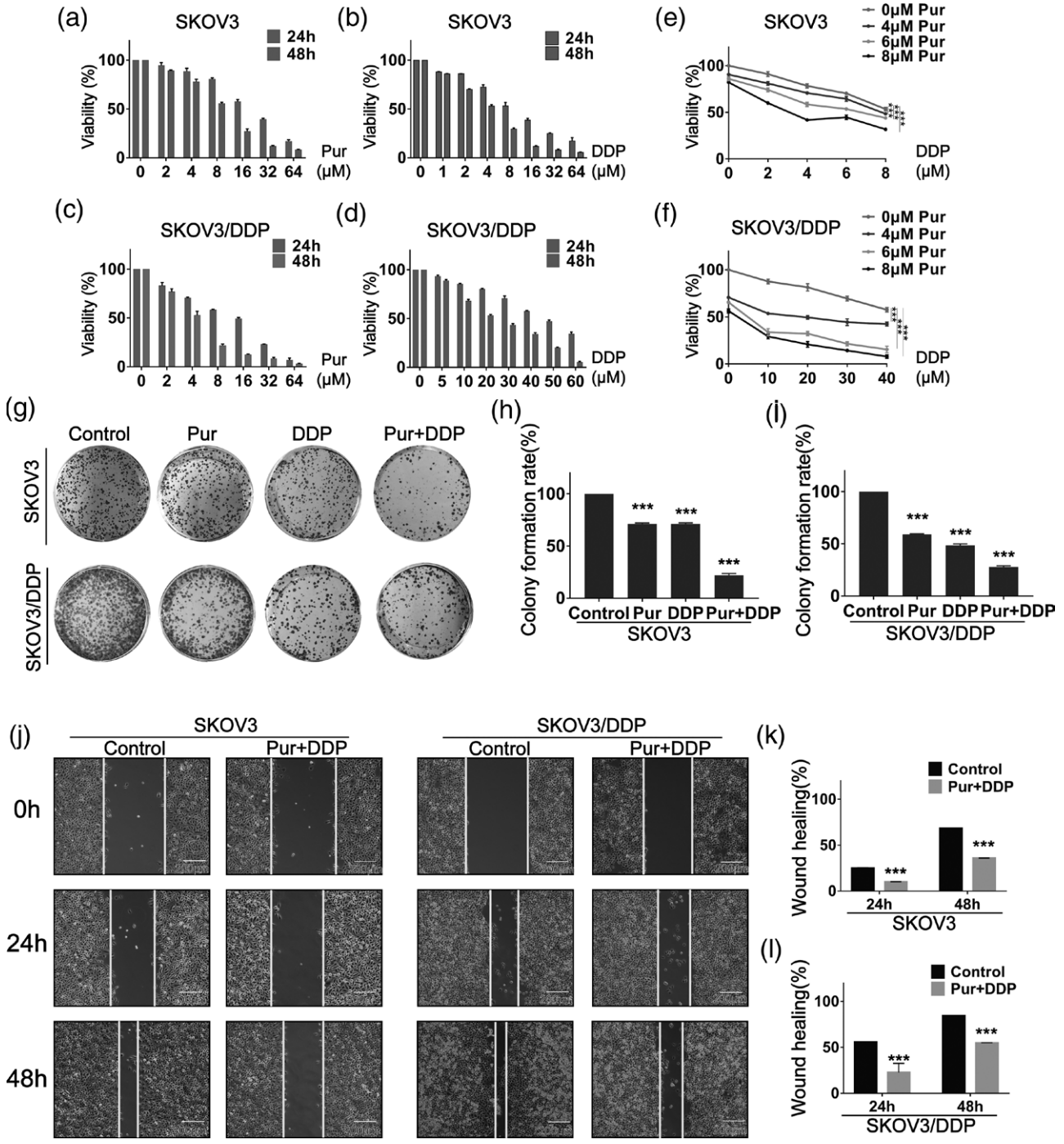

Pur and DDP exhibit an antiproliferation effect in SKOV3 and SKOV3/DDP cells. (a–d) Cells were incubated with various concentrations of Pur and DDP for 24 and 48 h, and cell viability was then determined by the CCK-8 assay. (e–f) Cells were incubated with different combination concentrations of Pur and DDP for 24 h, and cell viability was then determined by the CCK-8 assay. (g–i) Pur and DDP inhibited the colony formation ability of SKOV3 and SKOV3/DDP cells. (j–l) Wound healing assay showed the combination treatment of Pur and DDP inhibited EOC cells migration. Scale bar: 200 μm. The control group is the DMSO vehicle. All data are representative of three independent experiments. Bars, SEM. $n=3$ experiments. *$P<0.05$, **$P<0.01$, ***$P<0.001$. CCK-8, Cell Counting Kit-8; DMSO, dimethyl sulfoxide.

Mitochondrial membrane potential (ΔΨm) changes are critical incidents that take place during drug-induced apoptosis. After 24 h treatment with Pur, DDP, and Pur/DDP, the two EOC cells were stained with a fluorescent JC-1 probe. JC-1 accumulates and forms aggregations characterized by red fluorescence in the mitochondria and also

Table 1 **The combination index of Purvalanol A and cisplatin was calculated for the two epithelial ovarian cancer cell lines**

SKOV3				SKOV3/DDP			
DDP (μM)	Pur (μM)	Effect	CI	DDP (μM)	Pur (μM)	Effect	CI
2	4	0.23	0.922	10	4	0.526	0.664
4	4	0.28	0.802	20	4	0.485	0.954
6	4	0.308	0.768	30	4	0.53	0.981
8	4	0.291	0.958	40	4	0.561	1.026
2	6	0.214	1.416	10	6	0.72	0.45
4	6	0.305	0.952	20	6	0.671	0.644
6	6	0.366	0.757	30	6	0.789	0.441
8	6	0.515	0.417	40	6	0.847	0.355
2	8	0.618	0.35	10	8	0.711	0.594
4	8	0.587	0.398	20	8	0.822	0.398
6	8	0.527	0.504	30	8	0.87	0.323
8	8	0.622	0.359	40	8	0.925	0.213

CI, combination index; DDP, Cisplatin; Pur, Purvalanol A.

in the cytoplasm as a monomer characterized by green fluorescence. During apoptosis, the mitochondrial membrane is disturbed with depolarization of $\Delta\Psi m$ consequently, and JC-1 aggregates transform into monomers, which leads to the changes in the ratio of red to green fluorescence. The results showed that co-treated cells exhibited the most significant decline in red fluorescence and increase in green fluorescence (Fig. 3k and l). All these data demonstrated that the combined treatment of Pur and DDP was effective in inducing apoptosis in ovarian cancer cells.

The combination treatment of Pur and DDP causes cell cycle arrest in ovarian cancer cells

Given the critical role of CDK1 in the G1/S or G2/M Phases of the cell cycle, we then investigated the effect of Pur (with or without cisplatin) on cell-cycle progression. Two EOC cell lines were treated with Pur, DDP alone or in combination for 24 h, and cell-cycle analysis by flow cytometry showed that both Pur and Pur/DDP treatment resulted in an increased percentage of arrest in the G2/M phase compared with the control group. However, the application of DDP alone had no significant effect on cell-cycle progression in all EOC cell lines (Fig. 4a–d). We also investigated the expression levels of cell cycle-related proteins after treatment alone or combined. As shown in Fig. 4e–f, CDK1 expression was down-regulated following 24 h administration of Pur or Pur/DDP in EOC cells, whereas the alterations were NS in the DDP group.

Treatment of Pur with or without DDP induces autophagy in ovarian cancer cells

To investigate whether the combination treatment with Pur and DDP could trigger the pro-apoptotic effect of EOC cells by inducing autophagy, we performed western blot analysis to evaluate the protein levels of several autophagy markers. As shown in Fig. 5a–g, Pur/DDP combination treatment upregulated the expression of proteins including Beclin1, Atg3, Atg5, and Atg16 in EOC cells. Moreover, LC3-II, a classical autophagy marker, showed a striking increase in conversion in SKOV3 and SKOV3/DDP cells after Pur/DDP co-treatment. Furthermore, the expression of p62, another marker of autophagy, was decreased after Pur/DDP co-treatment compared with the control group. To dynamically track and quantify intracellular autophagic flux, we transfected tandem mRFP-GFP-LC3 adenovirus into SKOV3/DDP cells [36]. As shown in Fig. 5h and i, the quantity of detectable yellow autophagic LC3 puncta (mRFP+/GFP+) accumulated in the cytoplasm increased in the treated groups compared with the control group. Moreover, red puncta (mRFP+GFP–) containing mRFP-LC3 rather than green puncta (mRFP–GFP+) became preponderantly evident in cells undergoing the combined treatment. Collectively, our data demonstrated that the combined treatment could accumulate autophagosomes and autolysosomes, and activate complete autophagic flux in ovarian cancer cells.

Autophagy actually has widely different effects on tumor development and treatment, such as cytoprotective and pro-apoptotic. To evaluate whether combined treatment-induced autophagy is related to cell viability and apoptosis, we used 3-MA, an autophagy inhibitor, to block the autophagy process. First, western blot data showed that 3-MA decreased LC3-II protein expression and increased p62 protein levels in EOC cells (Fig. 5j–n), indicating that the autophagy induced by Pur/DDP co-treatment was attenuated. Subsequently, compared with Pur or DDP treatment alone, annexin V-PE/7-AAD assays showed that the combination of 3-MA with Pur/DDP significantly increased the number of apoptotic ovarian cancer cells (Fig. 5o). Correspondingly, the expression level of the pro-apoptotic protein Bax was upregulated, and the antiapoptotic protein Bcl-2 was downregulated after autophagy blockage (Fig. 5j–l). Taken together, these results suggested that the combination treatment of Pur/DDP with 3-MA enhanced the antitumor effect in ovarian cancer cells.

Elevation of reactive oxygen species generation in ovarian cancer cells by the combination of Pur and DDP is involved in apoptosis and autophagy by mediating the AKT/mTOR signaling pathway

Subsequently, to determine whether ROS accumulation is involved in combined treatment-induced apoptosis of EOC cells, we used the DCFH-DA probe to

Fig. 3

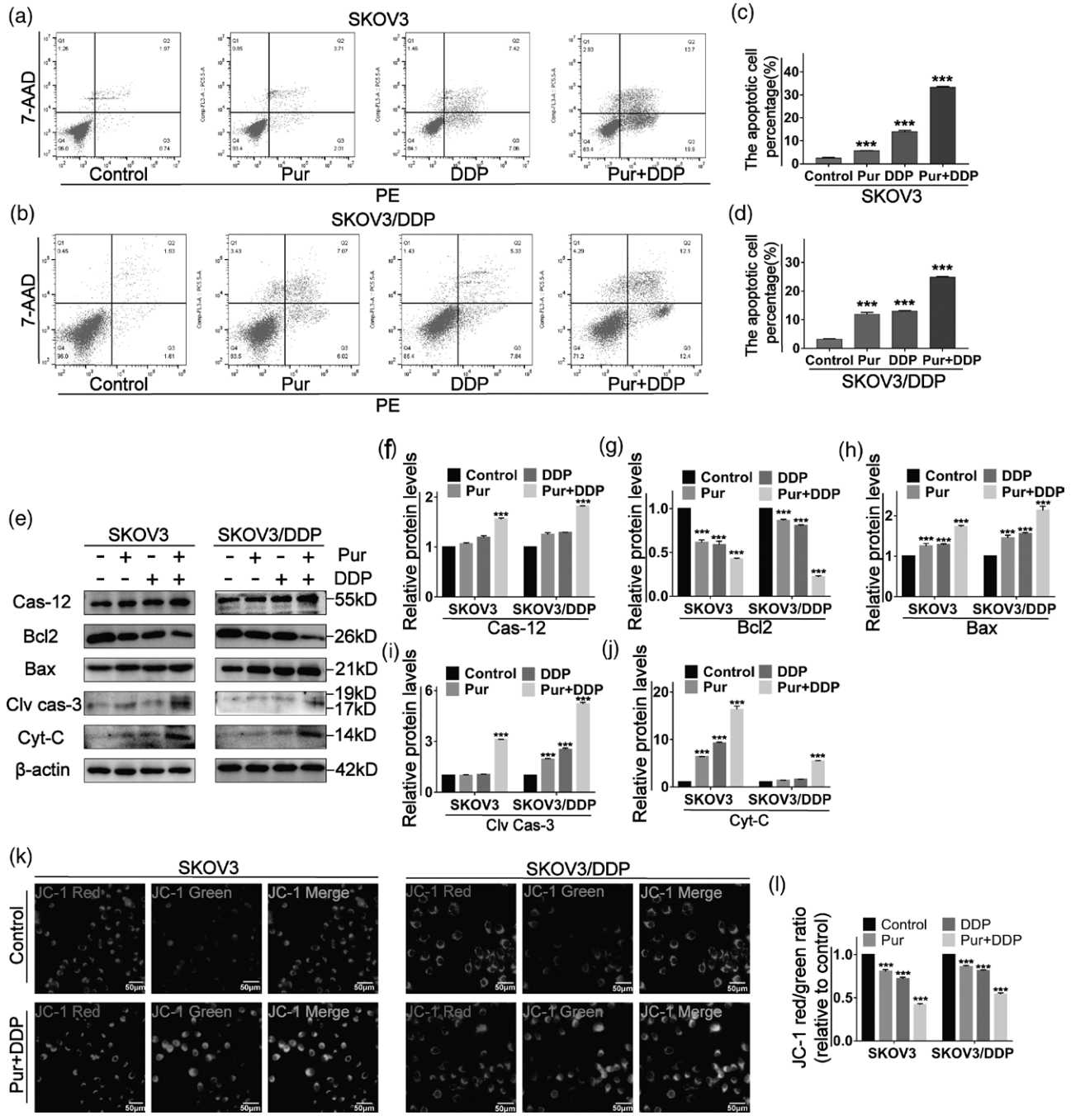

The combination treatment of Pur and DDP induces the apoptosis of ovarian cancer cells. (a–d) SKOV3 and SKOV3/DDP cells were treated with Pur (8 μM) or DDP (4 μM for SKOV3 cells and 30 μM for SKOV3/DDP cells) or in combination for 24 h, and then apoptotic cells were detected with the annexin V-PE/7-AAD kit and analyzed by flow cytometry. (e–j) the expression levels of apoptosis-related proteins in EOC cells including caspase-12, Bcl-2, Bax, cleaved caspase-3, and cytochrome-C were measured by western blotting. β-actin was included as a loading control. (k–l) The effects of Pur and DDP on alteration of the mitochondrial membrane potential ($\Delta\psi m$) in EOC cells were determined by JC-1 staining via fluorescence microscopy. Scale bar: 50 μm. All data are representative of three independent experiments. Bars, SEM. $n=3$ experiments. *$P<0.05$, **$P<0.01$, ***$P<0.001$ vs. the control (Pur-, DDP-). EOC, epithelial ovarian cancer; DDP, cisplatin; Pur, Purvalanol A.

investigate the intracellular ROS levels after exposure to Pur, DDP, and Pur/DDP combination. As shown in Fig. 6a and b, combination treatment resulted in a remarkable increase in ROS levels. We also measured SOD activity to estimate intracellular oxidative stress. As shown in Fig. 6c and d, treatment of cells with both

Fig. 4

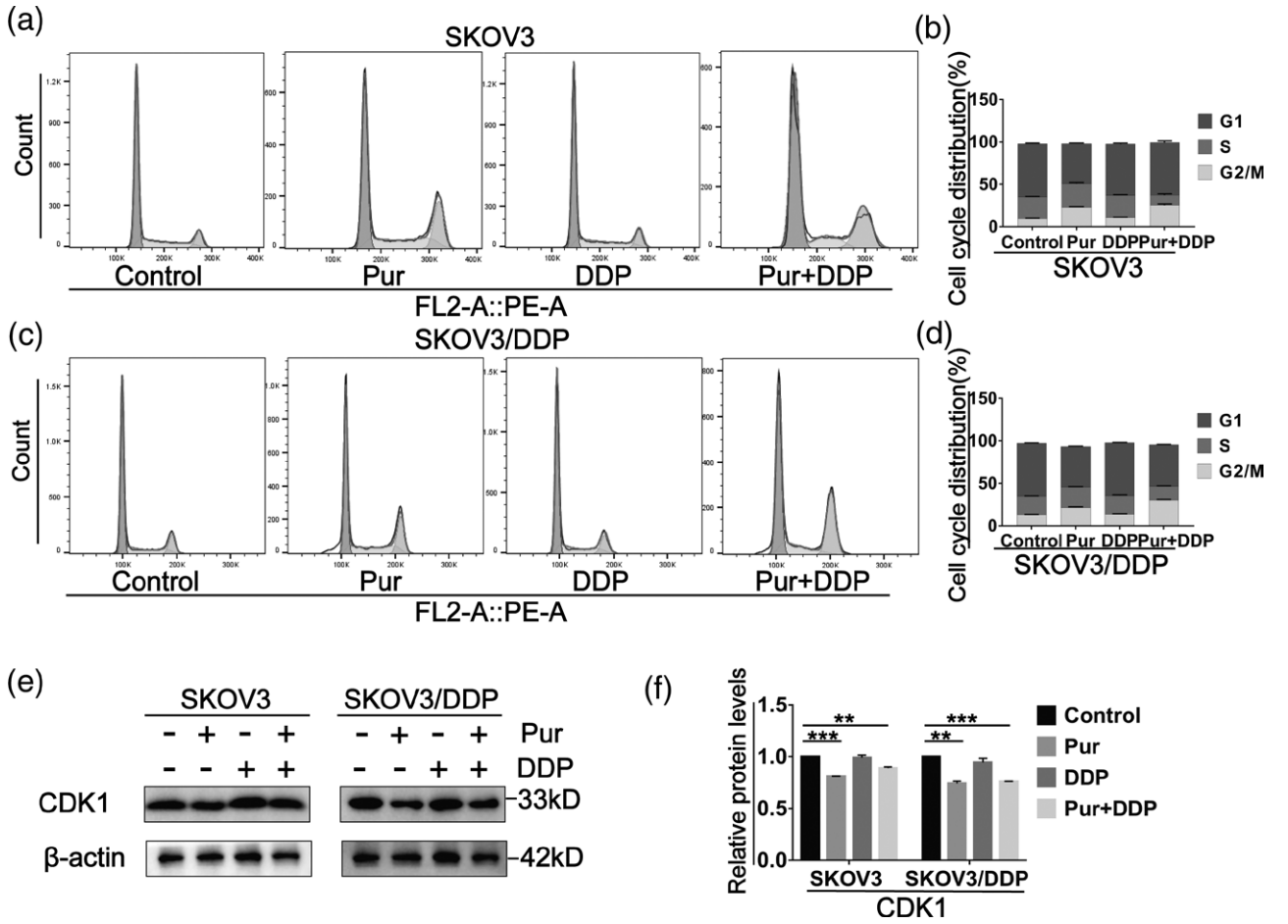

The combination treatment of Pur and DDP causes cell cycle arrest in ovarian cancer cells. SKOV3 and SKOV3/DDP cells were treated with Pur (8 μM) or DDP (4 μM for SKOV3 cells and 30 μM for SKOV3/DDP cells) or in combination for 24 h. (a–d) Cells were stained with PI and analyzed by flow cytometry. (e and f) The expression levels of CDK1 were measured by western blotting. β-actin was included as a loading control. All data are representative of three independent experiments. SEM. $n=3$ experiments. *$P<0.05$, **$P<0.01$, ***$P<0.001$ vs. the control (Pur- and DDP-). DDP, cisplatin; Pur, Purvalanol A.

Pur and DDP alone induced ascendant SOD activities, but the combined treatment exhibited the most significant increase. These results suggested that ROS accumulation might be a necessary event in the synergistic mechanism. Furthermore, pretreatment with NAC, a classic ROS scavenger markedly reversed the combined treatment-induced increase in ROS levels (Fig. 6a and b). Western blotting results showed that NAC pretreatment exceedingly downregulated the expression level of Bax and upregulated Bcl-2, correspondingly. In addition, the increase of autophagy-related marker LC3II/LC3I induced by combination treatment was also significantly attenuated in the presence of NAC (Fig. 6k). Likewise, the apoptosis induced by combination treatment in EOC cells was significantly abrogated after pretreatment with NAC (Fig. 6h–j). Overall, these results indicated the vital role of ROS in the synergistic effect of Pur and cisplatin.

Moreover, we detected whether the downregulation of the Akt/mTOR signaling pathway contributed to the apoptosis and autophagy of EOC cells induced by the combined treatment. Combined treatment downregulated the phosphorylation levels of Akt and mTOR, and NAC could partially reverse the reductions in p-Akt and p-mTOR induced by Pur/DDP combination treatment (Fig. 6e–p). In conclusion, our current results showed that the apoptosis and autophagy induced by the combination treatment of Pur and DDP in EOC cells could be mediated by elevated ROS through Akt/mTOR signaling pathway.

Pur and DDP inhibit tumor growth *in vivo*

To further investigate the inhibitory effect of Pur/DDP combination treatment *in vivo*, we established a xenograft model in immunodeficient mice. The xenograft mice were treated with normal saline, Pur

Fig. 5

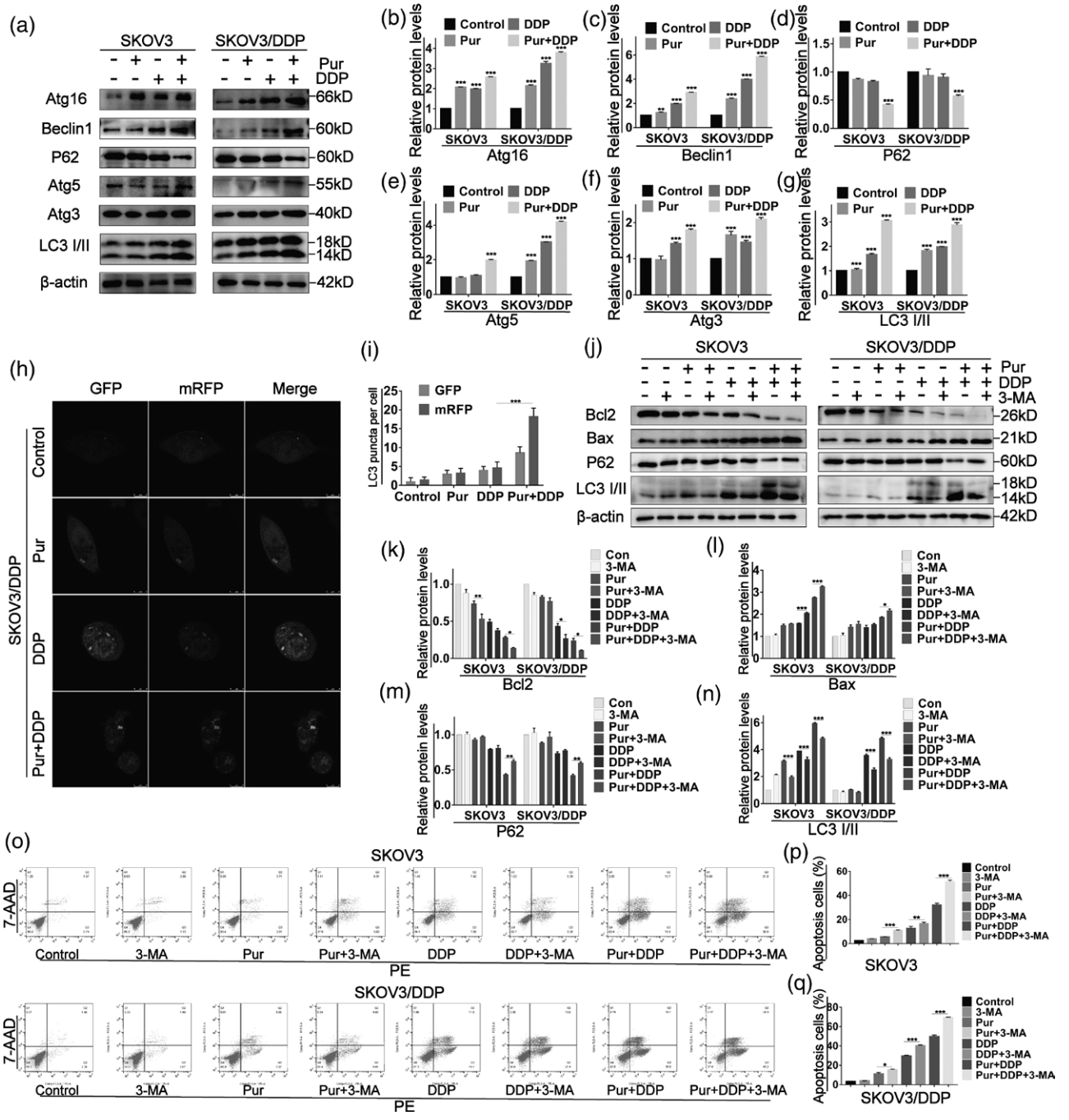

Treatment of Pur with or without DDP induce autophagy in ovarian cancer cells. SKOV3 and SKOV3/DDP cells were treated with Pur (8 μM) or DDP (4 μM for SKOV3 cells and 30 μM for SKOV3/DDP cells) or in combination for 24 h. (a–g) Western blot analysis of autophagy-related proteins such as Atg16, Beclin1, p62, Atg5, Atg3, and LC3II/LC3I in EOC cells. β-actin was included as a loading control. (h–i) SKOV3/DDP cells overexpressing mRFP-GFP-LC3 were treated with Pur (8 μM) or DDP (30 μM) or in combination for the indicated times and then subjected to confocal microscopy. Scale bar: 20 μm. The average numbers of green and red LC3 dots per cell in each condition were quantified, and over 30 cells were counted in each condition. The EOC cells were pretreated with 3-MA for 2 h prior to treatment with Pur and DDP alone or in combination for 24 h. (j–n). The expression of autophagy-related proteins including p62 and LC3 and apoptosis-related proteins including Bcl2 and Bax were analyzed by western blotting. β-actin was included as a loading control. (o–q) After pretreatment of 3-MA, apoptosis in EOC cells was determined by flow cytometry after staining with AnnexinV-FITC/PI. All data are representative of three independent experiments. Bars, SEM. $n=3$ experiments. *$P<0.05$, **$P<0.01$, ***$P<0.001$ vs. the control (Pur-, DDP-, and 3-MA-). DDP, cisplatin; 3-MA, 3-methyladenine; Pur, Purvalanol A; ROS, reactive oxygen species.

Fig. 6

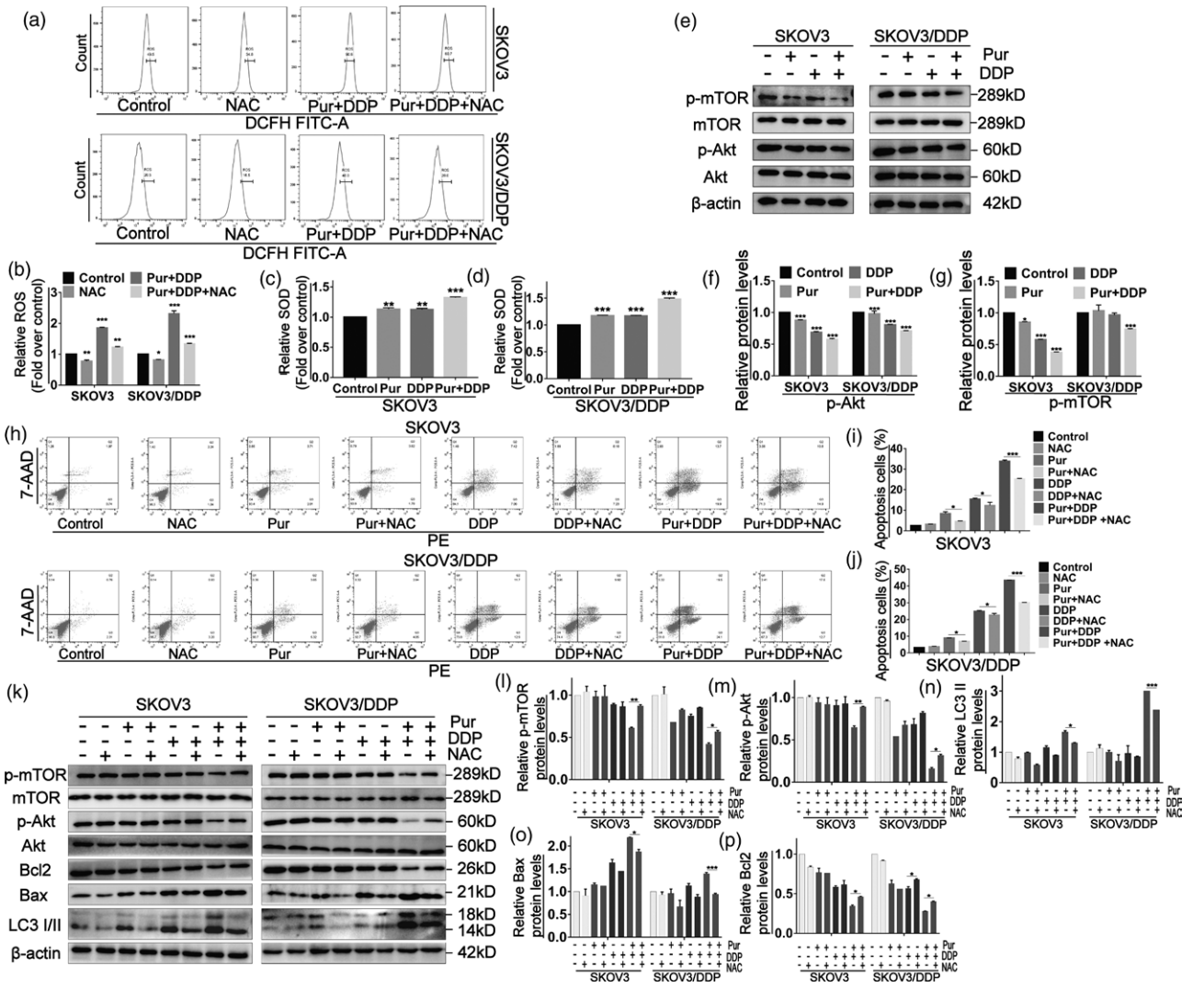

Elevation of ROS generation in ovarian cancer cells by the combination of Pur and DDP is involved in apoptosis and autophagy by mediating the AKT/mTOR signaling pathway. SKOV3 and SKOV3/DDP cells were pretreated with NAC (5 mM) for 2 h prior to the treatment of Pur (8 μM) or DDP (4 μM for SKOV3 cells and 30 μM for SKOV3/DDP cells) or in combination for 24 h. (a and b) The levels of cellular ROS were determined by flow cytometry after DCFH-DA (10 mM) staining. (c and d) SOD activities were determined by WST-1 assay. (e–g) The ROS/Akt/mTOR signaling pathway was measured by western blotting. (h–j) After ROS scavenging by NAC, the apoptosis percentage was determined by flow cytometry after staining with Annexin V-FITC/PI. (k–p) the expression levels of proteins involved in autophagy induction, apoptosis, and the Akt/mTOR signaling pathway were analyzed by western blotting. β-actin was included as a loading control. All data are representative of three independent experiments. Bars, SEM. $n=3$ experiments. *$P<0.05$, **$P<0.01$, ***$P<0.001$ vs. the control (Pur-, DDP-, and NAC-). DDP, cisplatin; NAC, N-acetylcysteine; Pur, Purvalanol A; ROS, reactive oxygen species.

(25 mg/kg), DDP (5 mg/kg), or the combination of Pur and DDP. As shown in Fig. 7a–c, tumor volume and weight were reduced in all treated groups, particularly in the combination treatment group. Besides, IHC staining of tumor specimens revealed that the combined treatment significantly increased the expression levels of LC3II/LC3I and decreased the protein levels of p-Akt and p-mTOR compared with the control group (Fig. 7d). These results suggested that the combination of Pur and DDP could significantly inhibit tumor growth *in vivo*, which was consistent with those in-vitro studies.

Discussion

DDP is one of the most widely used chemotherapeutic agents for the treatment of ovarian cancer, but its efficacy has been limited by the development of chemoresistance [37]. Combination treatment possesses a broad prospect of improving the efficacy of conventional treatment. Hence, finding new drugs to enhance the antitumor

effects of cisplatin or to reverse chemoresistance would provide a new line of attack.

The mammalian cell cycle is well-organized by different CDKs and their functional cyclin partners. Chemoresistance caused by aberrant activities of cell cycle proteins has become a great obstacle in cancer therapy, providing a theoretical basis for the study of cell cycle-related inhibitors [38]. CDK1 has previously been reported to be one of the master regulators of cancer growth and a key regulator for the cell cycle [39,40]. Dysregulated CDK1 activity has been frequently observed in cancers. A study on EOC demonstrated that elevated CDK1 expression in the cytoplasmic predicted low overall survival in EOC patients, and the inhibition of CDK1 expression and activity reduced ovarian cancer growth [41]. Other studies also reported that increased CDK1 expression and activity were found in colorectal, prostate, and lung cancer [42–44]. In our study, findings from the TCGA cohorts and GEO databases indicated that CDK1 was upregulated in ovarian cancer. K-M plots indicated that CDK1 levels were linked to poorer FIGO stages of EOC patients, in line with the oncogenic role for CDK1. Results of our study, together with previously reported findings, confirm that regulation of CDK1 is vital in the progression of cancer cells and that upregulation of CDK1 appears to contribute to the development and poorer differentiation of ovarian cancer.

Pur, which interdicts the binding of CDK1 with its specific cyclin counterpart, has shown a broad prospect of in-vitro anticancer activities. For instance, Pur suppressed the growth of human colon cancer cells [45], liver cancer cells [46], and breast cancer cells [21]. Our results showed that both Pur alone and DDP alone had inhibitory effects on EOC cells in a time- and dose-dependent manner. The CI values at combination regimens with Pur (8 μM) and DDP (4 μM for SKOV3 cells and 30 μM for SKOV3/DDP cells) at subtoxic concentrations were 0.398 and 0.323 separately, which indicated significant synergistic anticancer effects of Pur on EOC cells. In addition, we found that the combination treatment of Pur and DDP displayed a greater inhibitory effect on the viability, migration, and invasion of EOC cells. Moreover, we validated the effects of Pur and DDP *in vivo*, which further proved the combination treatment exhibited a distinct inhibitory effect on tumor growth. Previous studies have proven that Pur could act as a synergist in traditional cancer therapies. For example, a study of non-small cell lung cancer confirmed that Pur enhanced the cytotoxic effects of taxol in cancer cells [22]. Besides, the treatment with Pur resulted in a significant increase in radiation-induced gastric cancer cells death [47]. According to these data, we can infer that Pur suppresses the growth of cancer cells and enhance the cytotoxic effect of different anticancer agents in which DDP might be included, to reverse chemoresistance.

Autophagy exerts a paradoxical role in antineoplastic therapy since its complex and contradictory role in cancer [25]. The intimate interaction between cell cycle regulation and autophagy plays a key role in cellular homeostasis maintenance machinery [48]. Besides, it has been suggested that autophagy and apoptosis signaling pathways can interact with each other [49,50]. Recent research declared that both autophagy and apoptosis could be enhanced by Pur in colon cancer [20] and cervical cancer cells [51]. Therefore, clarifying the role of autophagy, and understanding the interaction between apoptosis and autophagy may be conducive to explaining the underlying synergistic mechanism of Pur in EOC. Similar to the research above, we demonstrated that both autophagy and apoptosis in EOC cells could be enhanced by Pur/DDP treatment in the present study. However, the number of ovarian cancer cells with apoptosis caused by 3-MA blocking autophagy increased significantly, strongly suggesting that Pur/DDP-induced autophagy may have a protective effect on EOC cells. Thus, autophagy inhibitors may be significant for ovarian cancer therapy if the combination treatment is used in the future.

The Akt/mTOR signaling pathway is one of the major survival pathways of tumor cells, and aberrant activation of the Akt/mTOR pathway is widely observed in various malignant tumors, which is involved in accelerating proliferation, promoting metastasis, and resistance to anticancer therapy [52–54]. Furthermore, it has been reported that Akt/mTOR signaling pathway negatively regulates autophagy, and the inhibition of the Akt/mTOR signaling pathway could directly stimulate autophagy and apoptosis [55]. In addition, growing evidence has shown that elevated ROS could regulate the AKT/mTOR signaling pathway [56,57]. A previous investigation has illustrated that Pur can selectively induce apoptosis in cancer cells by increasing intracellular ROS levels [51]. In a study on prostate cancer, Pur increased apoptosis and autophagy in prostate cancer cells by suppressing PI3K/Akt/mTOR pathway [58]. Similarly, our study found that the Pur/DDP combination treatment not only resulted in significant increases in ROS levels but also downregulated the Akt/mTOR signaling pathway in EOC cells. On the other hand, pretreatment with NAC significantly abolished the ROS increase and reversed the downregulation of the Akt/mTOR pathway. What is more, the combination treatment induced autophagy, and apoptosis was decreased by NAC as well. Thereby, the results above indicate that Pur combined with DDP can downregulate the Akt/mTOR signaling pathway in EOC cells by irritating oxidative stress, which may closely associate with cytoprotective autophagy and apoptosis in EOC cells.

Conclusion

In summary, our study demonstrated that Pur markedly enhanced the anti-tumor effect of DDP and induced apoptosis, autophagy, and cell cycle arrest in EOC cells,

Fig. 7

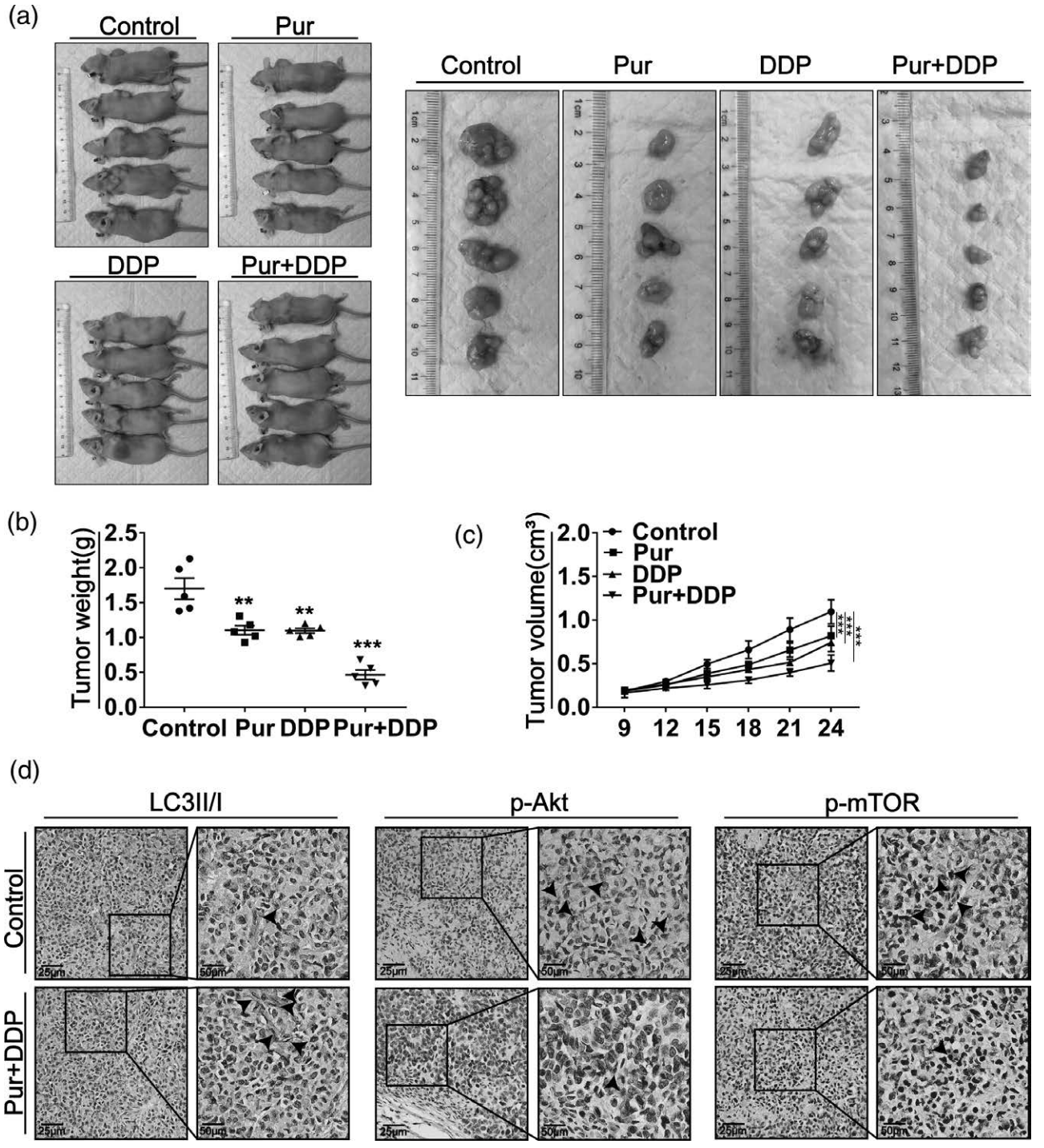

Pur and DDP inhibit tumor growth *in vivo*. Nude mice bearing xenograft tumors were treated with DMSO, Pur (25 mg/kg), DDP (5 mg/kg), or in combination. (a) Representative images of subcutaneous tumors after treatment ($n=5$). (b–c) The weights and volumes of the xenograft tumors were measured at the indicated time points. (d) LC3-I/II, p-Akt, and p-mTOR in the combination group tumor tissues compared with the control group were detected by IHC staining. Arrows indicate the LC3-I/II, p-Akt, or p-mTOR positive cells. Scale bar: 50 μm. Bars, SEM; $^{*}P<0.05$, $^{**}P<0.01$, $^{***}P<0.001$ vs. the control (Pur -, DDP-). DDP, Cisplatin; DMSO, dimethyl sulfoxide; mTOR, mammalian target of rapamycin; Pur, Purvalanol A; ROS, reactive oxygen species.

reversing the resistance to DDP in ovarian cancer. In addition, we found that the combined treatment induced apoptosis and cytoprotective autophagy by inhibiting the ROS/Akt/mTOR signaling pathway. These findings provide new insights into the molecular mechanisms of the synergistic effects of CDK inhibitors with DDP and suggest that such a combination treatment may be a promising strategy in ovarian cancer therapy.

Acknowledgements

The authors would like to thank all the teachers at the Department of Gynecology and Obstetrics and Central Laboratory, Renmin Hospital of Wuhan University, for their technical assistance in molecular biological experiments. The authors also would like to thank all the teachers at the Animal Experimental Center and Institute of Model Animal of Wuhan University, for their technical assistance in animal husbandry, animal breeding, and animal experiments.

This research is sponsored by the Second level fund of the second medical leading talents project of Hubei province (no. [2019]47) and the National Key Research and Development Program of China (2018YFC2002204).

Conflicts of interest

There are no conflicts of interest.

Reference

1 Torre LA, Trabert B, DeSantis CE, Miller KD, Samimi G, Runowicz CD, *et al*. Ovarian cancer statistics, 2018. *CA Cancer J Clin* 2018; **68**:284–296.
2 Lheureux S, Gourley C, Vergote I, Oza AM. Epithelial ovarian cancer. *Lancet* 2019; **393**:1240–1253.
3 Kuroki L, Guntupalli SR. Treatment of epithelial ovarian cancer. *BMJ* 2020; **371**:m3773.
4 Lheureux S, Braunstein M, Oza AM. Epithelial ovarian cancer: evolution of management in the era of precision medicine. *CA Cancer J Clin* 2019; **69**:280–304.
5 Ghosh S. Cisplatin: the first metal based anticancer drug. *Bioorg Chem* 2019; **88**:102925.
6 Aldossary SA. Review on pharmacology of cisplatin: clinical use, toxicity and mechanism of resistance of cisplatin. *Biomed Pharmacol J* 2019; **12**:7–15.
7 Roskoski R Jr. Cyclin-dependent protein serine/threonine kinase inhibitors as anticancer drugs. *Pharmacol Res* 2019; **139**:471–488.
8 Lemmens B, Lindqvist A. DNA replication and mitotic entry: a brake model for cell cycle progression. *J Cell Biol* 2019; **218**:3892–3902.
9 Mills CC, Kolb EA, Sampson VB. Development of chemotherapy with cell-cycle inhibitors for adult and pediatric cancer therapy. *Cancer Res* 2018; **78**:320–325.
10 Ingham M, Schwartz GK. Cell-cycle therapeutics come of age. *J Clin Oncol* 2017; **35**:2949–2959.
11 Asghar U, Witkiewicz AK, Turner NC, Knudsen ES. The history and future of targeting cyclin-dependent kinases in cancer therapy. *Nat Rev Drug Discov* 2015; **14**:130–146.
12 Chou J, Quigley DA, Robinson TM, Feng FY, Ashworth A. Transcription-associated cyclin-dependent kinases as targets and biomarkers for cancer therapy. *Cancer Discov* 2020; **10**:351–370.
13 Otto T, Sicinski P. Cell cycle proteins as promising targets in cancer therapy. *Nat Rev Cancer* 2017; **17**:93–115.
14 Yasukawa M, Ando Y, Yamashita T, Matsuda Y, Shoji S, Morioka MS, *et al*. CDK1 dependent phosphorylation of hTERT contributes to cancer progression. *Nat Commun* 2020; **11**:1557.
15 Chen S, Chen X, Xiu YL, Sun KX, Zhao Y. MicroRNA-490-3P targets CDK1 and inhibits ovarian epithelial carcinoma tumorigenesis and progression. *Cancer Lett* 2015; **362**:122–130.
16 Xie B, Wang S, Jiang N, Li JJ. Cyclin B1/CDK1-regulated mitochondrial bioenergetics in cell cycle progression and tumor resistance. *Cancer Lett* 2019; **443**:56–66.
17 Kumar SK, LaPlant B, Chng WJ, Zonder J, Callander N, Fonseca R, *et al*; Mayo Phase 2 Consortium. Dinaciclib, a novel CDK inhibitor, demonstrates encouraging single-agent activity in patients with relapsed multiple myeloma. *Blood* 2015; **125**:443–448.
18 Au-Yeung G, Lang F, Azar WJ, Mitchell C, Jarman KE, Lackovic K, *et al*. Selective targeting of cyclin E1-amplified high-grade serous ovarian cancer by cyclin-dependent kinase 2 and AKT inhibition. *Clin Cancer Res* 2017; **23**:1862–1874.
19 Chohan TA, Qayyum A, Rehman K, Tariq M, Akash MSH. An insight into the emerging role of cyclin-dependent kinase inhibitors as potential therapeutic agents for the treatment of advanced cancers. *Biomed Pharmacother* 2018; **107**:1326–1341.
20 Coker-Gürkan A, Arisan ED, Obakan P, Akalın K, Özbey U, Palavan-Unsal N. Purvalanol induces endoplasmic reticulum stress-mediated apoptosis and autophagy in a time-dependent manner in HCT116 colon cancer cells. *Oncol Rep* 2015; **33**:2761–2770.
21 Obakan P, Arısan ED, Özfiliz P, Çoker-Gürkan A, Palavan-Ünsal N. Purvalanol A is a strong apoptotic inducer via activating polyamine catabolic pathway in MCF-7 estrogen receptor positive breast cancer cells. *Mol Biol Rep* 2014; **41**:145–154.
22 Chen X, Liao Y, Long D, Yu T, Shen F, Lin X. The Cdc2/Cdk1 inhibitor, purvalanol A, enhances the cytotoxic effects of taxol through Op18/stathmin in non-small cell lung cancer cells *in vitro*. *Int J Mol Med* 2017; **40**:235–242.
23 Mizushima N, Komatsu M. Autophagy: renovation of cells and tissues. *Cell* 2011; **147**:728–741.
24 Levy JMM, Towers CG, Thorburn A. Targeting autophagy in cancer. *Nat Rev Cancer* 2017; **17**:528–542.
25 White E. The role for autophagy in cancer. *J Clin Invest* 2015; **125**:42–46.
26 Xu Z, Han X, Ou D, Liu T, Li Z, Jiang G, *et al*. Targeting PI3K/AKT/mTOR-mediated autophagy for tumor therapy. *Appl Microbiol Biotechnol* 2020; **104**:575–587.
27 Kumar D, Shankar S, Srivastava RK. Rottlerin induces autophagy and apoptosis in prostate cancer stem cells via PI3K/Akt/mTOR signaling pathway. *Cancer Lett* 2014; **343**:179–189.
28 Scherz-Shouval R, Elazar Z. Regulation of autophagy by ROS: physiology and pathology. *Trends Biochem Sci* 2011; **36**:30–38.
29 Sosa V, Moliné T, Somoza R, Paciucci R, Kondoh H, LLeonart ME. Oxidative stress and cancer: an overview. *Ageing Res Rev* 2013; **12**:376–390.
30 Gorrini C, Harris IS, Mak TW. Modulation of oxidative stress as an anticancer strategy. *Nat Rev Drug Discov* 2013; **12**:931–947.
31 Alzahrani AS. PI3K/Akt/mTOR inhibitors in cancer: at the bench and bedside. *Semin Cancer Biol* 2019; **59**:125–132.
32 Ediriweera MK, Tennekoon KH, Samarakoon SR. Role of the PI3K/AKT/mTOR signaling pathway in ovarian cancer: biological and therapeutic significance. *Semin Cancer Biol* 2019; **59**:147–160.
33 Burris HA 3rd. Overcoming acquired resistance to anticancer therapy: focus on the PI3K/AKT/mTOR pathway. *Cancer Chemother Pharmacol* 2013; **71**:829–842.
34 Deng J, Bai X, Feng X, Ni J, Beretov J, Graham P, Li Y. Inhibition of PI3K/Akt/mTOR signaling pathway alleviates ovarian cancer chemoresistance through reversing epithelial-mesenchymal transition and decreasing cancer stem cell marker expression. *BMC Cancer* 2019; **19**:618.
35 Chou TC. Drug combination studies and their synergy quantification using the Chou-Talalay method. *Cancer Res* 2010; **70**:440–446.
36 Gao L, Wang Z, Lu D, Huang J, Liu J, Hong L. Paeonol induces cytoprotective autophagy via blocking the Akt/mTOR pathway in ovarian cancer cells. *Cell Death Dis* 2019; **10**:609.
37 van Zyl B, Tang D, Bowden NA. Biomarkers of platinum resistance in ovarian cancer: what can we use to improve treatment. *Endocr Relat Cancer* 2018; **25**:R303–R318.
38 Pang W, Li Y, Guo W, Shen H. Cyclin E: a potential treatment target to reverse cancer chemoresistance by regulating the cell cycle. *Am J Transl Res* 2020; **12**:5170–5187.
39 Santamaría D, Barrière C, Cerqueira A, Hunt S, Tardy C, Newton K, *et al*. Cdk1 is sufficient to drive the mammalian cell cycle. *Nature* 2007; **448**:811–815.
40 Malumbres M, Barbacid M. Cell cycle, CDKs and cancer: a changing paradigm. *Nat Rev Cancer* 2009; **9**:153–166.
41 Yang W, Cho H, Shin HY, Chung JY, Kang ES, Lee EJ, Kim JH. Accumulation of cytoplasmic CDK1 is associated with cancer growth and survival rate in epithelial ovarian cancer. *Oncotarget* 2016; **7**:49481–49497.

42 Sung WW, Lin YM, Wu PR, Yen HH, Lai HW, Su TC, *et al*. High nuclear/cytoplasmic ratio of CDK1 expression predicts poor prognosis in colorectal cancer patients. *BMC Cancer* 2014; **14**:951.

43 Willder JM, Heng SJ, McCall P, Adams CE, Tannahill C, Fyffe G, *et al*. Androgen receptor phosphorylation at serine 515 by CDK1 predicts biochemical relapse in prostate cancer patients. *Br J Cancer* 2013; **108**:139–148.

44 Li M, He F, Zhang Z, Xiang Z, Hu D. CDK1 serves as a potential prognostic biomarker and target for lung cancer. *J Int Med Res* 2020; **48**:300060519897508.

45 Hikita T, Oneyama C, Okada M. Purvalanol A, a CDK inhibitor, effectively suppresses Src-mediated transformation by inhibiting both CDKs and c-Src. *Genes Cells* 2010; **15**:1051–1062.

46 Novotná E, Büküm N, Hofman J, Flaxová M, Kouklíková E, Louvarová D, Wsól V. Roscovitine and purvalanol A effectively reverse anthracycline resistance mediated by the activity of aldo-keto reductase 1C3 (AKR1C3): a promising therapeutic target for cancer treatment. *Biochem Pharmacol* 2018; **156**:22–31.

47 Iizuka D, Inanami O, Kashiwakura I, Kuwabara M. Purvalanol A enhances cell killing by inhibiting up-regulation of CDC2 kinase activity in tumor cells irradiated with high doses of X rays. *Radiat Res* 2007; **167**:563–571.

48 Zheng K, He Z, Kitazato K, Wang Y. Selective autophagy regulates cell cycle in cancer therapy. *Theranostics* 2019; **9**:104–125.

49 Maiuri MC, Zalckvar E, Kimchi A, Kroemer G. Self-eating and self-killing: crosstalk between autophagy and apoptosis. *Nat Rev Mol Cell Biol* 2007; **8**:741–752.

50 Gump JM, Thorburn A. Autophagy and apoptosis: what is the connection? *Trends Cell Biol* 2011; **21**:387–392.

51 Ozfiliz-Kilbas P, Sarikaya B, Obakan-Yerlikaya P, Coker-Gurkan A, Arisan ED, Temizci B, Palavan-Unsal N. Cyclin-dependent kinase inhibitors, roscovitine and purvalanol, induce apoptosis and autophagy related to unfolded protein response in HeLa cervical cancer cells. *Mol Biol Rep* 2018; **45**:815–828.

52 Fresno Vara JA, Casado E, de Castro J, Cejas P, Belda-Iniesta C, González-Barón M. PI3K/Akt signalling pathway and cancer. *Cancer Treat Rev* 2004; **30**:193–204.

53 Blume-Jensen P, Hunter T. Oncogenic kinase signalling. *Nature* 2001; **411**:355–365.

54 LoPiccolo J, Blumenthal GM, Bernstein WB, Dennis PA. Targeting the PI3K/Akt/mTOR pathway: effective combinations and clinical considerations. *Drug Resist Updat* 2008; **11**:32–50.

55 Rong L, Li Z, Leng X, Li H, Ma Y, Chen Y, Song F. Salidroside induces apoptosis and protective autophagy in human gastric cancer AGS cells through the PI3K/Akt/mTOR pathway. *Biomed Pharmacother* 2020; **122**:109726.

56 Zhao Z, Zhang P, Li W, Wang D, Ke C, Liu Y, *et al*. Pegylated recombinant human arginase 1 induces autophagy and apoptosis via the ROS-Activated AKT/mTOR pathway in bladder cancer cells. *Oxid Med Cell Longev* 2021; **2021**:5510663.

57 Zhao S, Cheng L, Shi Y, Li J, Yun Q, Yang H. MIEF2 reprograms lipid metabolism to drive progression of ovarian cancer through ROS/AKT/mTOR signaling pathway. *Cell Death Dis* 2021; **12**:18.

58 Berrak O, Arisan ED, Obakan-Yerlikaya P, Coker-Gürkan A, Palavan-Unsal N. mTOR is a fine tuning molecule in CDK inhibitors-induced distinct cell death mechanisms via PI3K/AKT/mTOR signaling axis in prostate cancer cells. *Apoptosis* 2016; **21**:1158–1178.